

Magneto-Acoustic Spectroscopy in Superfluid $^3\text{He-B}$

J.P. Davis, H. Choi, J. Pollanen, and W.P. Halperin

Department of Physics and Astronomy, Northwestern University, Evanston, Illinois 60208

(Dated: Version October 14, 2021)

We have used the recently discovered acoustic Faraday effect in superfluid ^3He to perform high resolution spectroscopy of an excited state of the superfluid condensate. With acoustic cavity interferometry we measure the rotation of the plane of polarization of a transverse sound wave propagating in the direction of magnetic field from which we determine the Zeeman energy of the excited state. We interpret the Landé g -factor, combined with the zero-field energies of the state, using the theory of Sauls and Serene to calculate the strength of f -wave interactions in ^3He .

PACS numbers: 67.57.Jj, 43.35.Rw, 74.20.Rp

Magneto-acoustic effects are less commonly known than their magneto-optical counterparts, but similar phenomena occur with transverse sound if there is significant magneto-elastic coupling. An acoustic Faraday effect (AFE) was first predicted for ferromagnetic crystals by Kittel [1] and subsequently was observed in magnetically ordered materials [2, 3]. It may also occur in the vortex lattice of high- T_c superconductors [4]. At low temperature in the superfluid state of ^3He , the spontaneously broken relative spin-orbit symmetry of the B-phase provides the mechanism for such a coupling. An AFE was predicted by Moores and Sauls [5] and observed by Lee *et al.* [6] proving that transverse sound waves exist in superfluid ^3He . It is of special note that this is the only known case where transverse waves propagate in a fluid. With recent improvements in acoustic cavity techniques [7] we have achieved sufficiently high spectroscopic resolution over a wide range of frequency to measure the AFE and study the excited states of the condensate as a function of pressure. The pressure is an essential variable that permits one to vary the strength of quasiparticle and pairing interactions. Using the theory of Sauls and Serene [8] we relate our Faraday rotation results to these interactions.

The acoustic Faraday effect requires two coupled modes; a transverse-sound mode, linearly-dispersive in the absence of magneto-elastic coupling, with phase velocity $c = \omega/q$ for frequency ω at wave vector q . The second mode must be magnetically active, $\omega^2 = \Omega_0^2(H) + bq^2$, having a magnetic field dependence in the long wavelength limit and quadratic dispersion. For ordered materials Ω_0 is the ferro- or antiferromagnetic resonance frequency, proportional to the internal local field and shifted linearly by an applied field, H . For superfluid ^3He the magnetic mode, Ω_{2-} , is an excited state of the superfluid condensate, having total angular momentum $J = 2$, called the *imaginary* squashing collective mode (ISQ), a reference to the nature of the order parameter distortions that characterize it, and to distinguish it from another $J = 2$ mode that involves only *real* components of the order parameter [9]. The linear Zeeman splitting of the ISQ-mode is the source of the magnetic field dependence, which leads to different couplings for right and left circularly polarized transverse sound, i.e. acoustic circular birefringence.

The coupled-mode dispersion relation for superfluid ^3He in

the long wavelength limit [5, 10] can be written as,

$$\frac{\omega^2}{q^2 v_F^2} = \Lambda_0 + \Lambda_{2-} \frac{\omega^2}{\omega^2 - \Omega_{2-}^2 - \frac{2}{5} q^2 v_F^2 - 2m_J g_{2-} \gamma_{eff} H \omega}, \quad (1)$$

where γ_{eff} is the effective gyromagnetic ratio of ^3He , m_J is the total angular momentum substate quantum number, and v_F is the Fermi velocity. The ISQ-mode frequency follows the temperature and pressure dependence of the energy gap, $\Delta(T, P)$, shown in Fig. 1, or more precisely $\Omega_{2-}^2 = a_{2-}^2 \Delta^2$, where $a_{2-} \approx \sqrt{12/5}$. The first term in Eq. 1 is a quasi-particle background, $\Lambda_0 = \frac{F_1^s}{15} (1 - \lambda) (1 + \frac{F_2^s}{5}) / (1 + \lambda \frac{F_2^s}{5})$. The magneto-acoustic coupling strength is $\Lambda_{2-} = \frac{2F_1^s}{75} \lambda (1 + \frac{F_2^s}{5})^2 / (1 + \lambda \frac{F_2^s}{5})$ for right and left circularly polarized sound waves ($m_J = \pm 1$). The Tsuneto function $\lambda(\omega, T)$ can be calculated from the energy gap [5]. The Fermi liquid parameterization of quasiparticle interactions is given in terms of $F_{1,2}^s$. Both a_{2-} and the Landé g -factor, g_{2-} , are predicted to

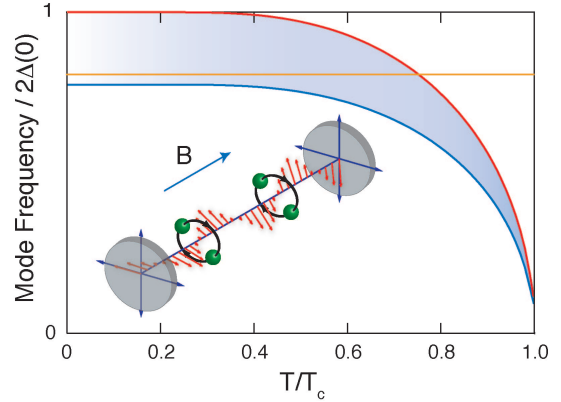


FIG. 1: (color online). The ISQ-mode frequency (lower blue curve) and pair-breaking (upper red curve) relative to the zero temperature gap as a function of temperature. Propagation of transverse sound, generated at constant frequency (orange line), is observed in the shaded (blue) region. The cartoon shows the acoustic Faraday effect, in which linearly polarized transverse waves (red arrows) are generated by a piezoelectric transducer and rotated by a magnetic field. The green spheres represent ^3He Cooper pairs coupling to transverse sound.

depend on the strength of quasiparticle and f -wave pairing interactions and consequently on temperature and pressure. In this letter we present our measurements of the Faraday rotation angle from which we determine the g -factor. From our results, along with accurate measurements of a_{2-} [7], we are able to determine the f -wave pairing interaction strength.

We cool the liquid ^3He by adiabatic nuclear demagnetization to temperatures $\approx 500 \mu\text{K}$. These methods, including thermometry, are described elsewhere [11]. A cavity for liquid ^3He is formed using an AC-cut quartz transducer as one wall with an optically polished quartz reflector as the other. The spacing is defined by two wires with diameter $\approx 25 \mu\text{m}$. Spring loading this cavity ensures that the cavity walls are parallel and that the spacing is uniform over the entire area of the cavity even as the experiment is cooled to low temperatures. The spacing was measured at room temperature using fluorescence techniques on a Zeiss Meta 500 confocal laser microscope at many places over its area. At 18 mK, $D = 31.6 \pm 0.1 \mu\text{m}$ was determined from the known dependence of the longitudinal sound velocity on pressure [9]. We use overtone frequencies, odd harmonics between 13 and 27, in the range 76 MHz to 159 MHz.

As the phase velocity of transverse sound changes so does the number of half-wavelengths in the cavity, altering the acoustic impedance at the surface of the piezoelectric transducer and producing a shift in the resonance spectrum which we detect with a resolution of $\approx 2 \times 10^{-6}$ using an RF-bridge, FM-modulation, and lock-in detection [7, 11]. In our experiment we hold ω constant and sweep either the temperature or pressure to vary the ISQ-mode frequency, Ω_{2-} (see Fig. 1). We detect the changing velocity as an oscillatory acoustic re-

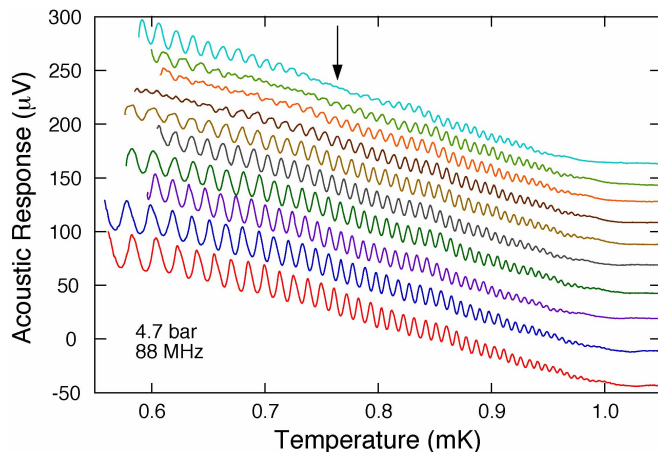


FIG. 2: (color online). Acoustic cavity response as a function of temperature for 4.7 bar and 88 MHz. Each trace (offset for clarity) is for a different magnetic field, bottom to top: 0, 61, 91, 122, 152, 183, 244, 274, 305 and 366 G. As the magnetic field is increased the linear polarization of transverse sound is rotated, decreasing the amplitude of the interference oscillations. At 366 G it is clear that there is a minimum (vertical arrow) in the acoustic response at 765 μK , which corresponds to a $\pi/2$ rotation of the polarization of the reflected wave with respect to the detection and generation direction.

sponse, displayed in Fig. 2. Precise changes of the velocity can be measured and by comparison with Eq. 1 near the ISQ-mode [12], we have determined their absolute values. We find that the phase velocity approaches 500 m/s close to the mode, so that it in this limit the first term in Eq. 1, Λ_0 , is negligible.

It is expected [5] that off-resonant coupling of transverse sound to the ISQ-mode holds only in the shaded region of Fig. 1. Otherwise propagation is strongly attenuated, either by pair breaking, $\omega > 2\Delta$, or if $\omega < \Omega_{2-}$. In the latter case there are no real-valued solutions for q in Eq. 1. In our previous work [7], extended here to 27 bar, we used the acoustic signature for $\omega = \Omega_{2-}(T, P)$ to obtain $\Omega_{2-}(0, P) = \sqrt{12/5}(1.0018 + 0.00144P)\Delta^+(0, P) \pm 0.3\%$. These results are expressed in terms of the weak-coupling-plus gap [9, 13], $\Delta^+(T, P)$, fixed to the Greywall temperature scale [14]. Additionally, we find that some harmonics of AC-cut transducers can generate *longitudinal* acoustic cavity resonances giving oscillatory acoustic response immediately below the shaded region in Fig. 1. We reported this earlier [7] although, at the time, we were unaware of its origin.

The acoustic Faraday effect is schematically represented in Fig. 1. Application of a magnetic field splits the ISQ-mode into five components. One of these, $m_J = 1$, couples to right circularly polarized sound and its frequency is increased by field. A second, $m_J = -1$, couples to left circular sound and is decreased by field. Consequently, these circularly polarized waves have different phase velocities. They interfere and thus rotate the plane of linear polarization proportional to path length and to the applied magnetic field, directly analogous to the magneto-optic effect discovered by Michael Faraday.

To accurately measure the AFE rotation angle, we slowly sweep either the temperature or pressure at constant frequency in various magnetic fields applied along the direction of propagation. For temperature sweeps this corresponds to the horizontal line in Fig. 1, typically in the range of ≈ 500 to 900 μK . Acoustic response data for temperature sweeps in different magnetic fields are shown in Fig. 2, which we can represent in the form,

$$A = A_0 + A_1 \cos \theta \sin(2D\omega/c + \phi), \quad (2)$$

where $\theta = \frac{\pi}{2}(H/H_{\pi/2})$ is the Faraday rotation angle, $H_{\pi/2}$ is the field that rotates the polarization by $\pi/2$ and ϕ is a phase. The $\cos \theta$ factor is the projection of the rotated polarization with respect to a fixed direction of polarization for generation and detection of transverse sound, characteristic of the transducer. A_0 is a smoothly varying background signal in the absence of acoustic cavity interference; A_1 is the maximum signal modulation from acoustic interference in the cavity. The rapid oscillatory behavior in Fig. 2 comes from the temperature dependence of the phase velocity, modulated by the field dependence of the Faraday rotation angle. Typical results are shown in Fig. 3 for $P = 4.7$ bar, $T = 626 \mu\text{K}$ and a frequency of 88 MHz.

The amplitude of the oscillations in the acoustic response in Fig. 2 decreases as the magnetic field is increased at fixed temperature, passing through a minimum indicated, for example,

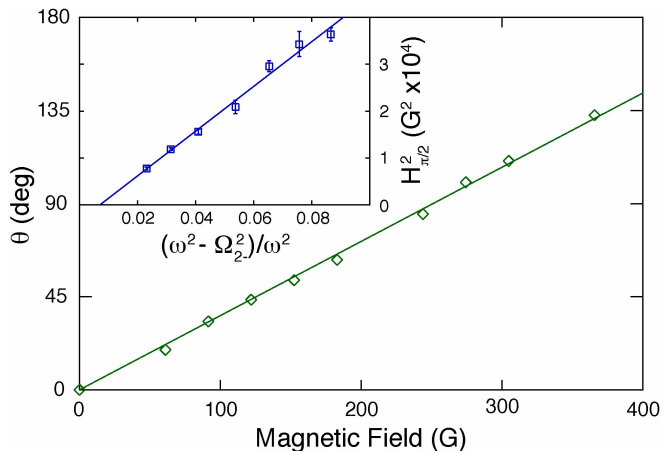


FIG. 3: (color online). The Faraday rotation angle as a function of applied field H for representative data at $P = 4.7$ bar, $T = 626$ μ K and frequency 88 MHz. (Inset) The square of the field for a $\pi/2$ Faraday rotation angle, $H_{\pi/2}^2$, is shown as a function of proximity to the ISQ-mode, $\Omega_{2-}(P)$, extrapolated to $T = 0$; with a frequency of 135.1 MHz and centered around 17.3 bar.

by an arrow in Fig. 2 at 366 G and 765 μ K. This corresponds to a $\pi/2$ rotation of the linear polarization as the wave traverses a round-trip path in the cavity. From the data in Fig. 2 we find θ at constant temperature and plot its dependence on magnetic field in Fig. 3. We find that the rotation angle is proportional to magnetic field for all pressures.

It is convenient to work at the lowest temperatures to minimize temperature dependences, so we extrapolate our measurements of $H_{\pi/2}(T)$ to $T = 0$ using a phenomenological expression that fits our data well, $H_{\pi/2}(T) = H_{\pi/2}(0) + B e^{-2\Delta(0)/k_B T}$, where B is a fit parameter. An example of these results, inset to Fig. 3, shows that for acoustic frequencies approaching the ISQ-mode, $H_{\pi/2}(0)$ becomes smaller, increasing the Faraday rotation angle in a fixed field.

Quantitative comparison with theory [10] requires that we calculate the g -factor in terms of $H_{\pi/2}$, using the condition for $\pi/2$ rotation, $q_+ - q_- = \frac{\pi}{2D}$ where q_{\pm} corresponds to $m_J = \pm 1$ in Eq. 1. We show that sufficiently close to the ISQ-mode,

$$g_{2-} = \sqrt{\frac{\omega^2 - \Omega_{2-}^2}{\omega^2}} \frac{v_F \Lambda_{2-}^{1/2}}{\gamma_{eff} H_{\pi/2} 8D}. \quad (3)$$

Determination of g_{2-} depends on precise knowledge of the ISQ-mode frequency, Ω_{2-} as defined above, which we have measured independently in zero field. This formulation for magneto-acoustics follows from the dispersion relation, Eq. 1, which can be verified experimentally. We have performed seven measurements of $H_{\pi/2}(0)$ at a single acoustic frequency of 135.1 MHz within a small pressure range from $P = 16.4$ to 18.2 bar, that tunes the ISQ-mode frequency from 129.1 to 133.5 MHz (over which the variation in g_{2-} is small). Our results in the inset of Fig. 3 are a validation of the predicted frequency behavior in Eq. 3. An unconstrained linear fit to the

data has a small offset that corresponds to a shift in ISQ-mode frequency of 0.3% which is within experimental error.

Eq. 3 is accurate when the difference between the acoustic frequency and the ISQ-mode frequency is small, which is valid for some of our data. Outside of this limit the quasiparticle term, Λ_0 , as well as the dispersion term, $\frac{2}{5} q^2 v_F^2$, become non-negligible and must be taken into account. Accordingly, we have calculated g_{2-} from $H_{\pi/2}(0)$ using the full dispersion relation in Eq. 1, which is solved numerically. This is performed for all of our data and the resulting g_{2-} values are presented in Fig. 4.

A second method for data acquisition is to sweep the pressure at our lowest possible temperature, ≈ 500 μ K, for various applied magnetic fields. In this case the pressure dependence of the transverse velocity is responsible for oscillatory acoustic response similar to that shown for temperature sweeps, as in Fig. 2. From these measurements we obtain $H_{\pi/2}(0)$ and, as described above, determine the values for g_{2-} shown as black squares in Fig. 4. There is good agreement between the two methods.

Our results for g_{2-} cover the full pressure range of superfluid $^3\text{He-B}$. The theoretical value for $g_{2-}(T = 0)$ without the effects of F_2^s or f -wave interactions is 0.0372 [8, 15]. A previous result, shown as a green diamond in Fig. 4, by Lee *et al.* [6] from the AFE at 4.4 bar, agrees qualitatively with our work, where the difference can be ascribed to less accuracy in their determination of Ω_{2-} . Movshovich *et al.* [16] used longitudinal acoustics at much higher magnetic fields to directly determine the ISQ-mode splitting. Their considerably higher result, shown as a blue triangle, is likely due to non-linear magnetic field dependence of the mode frequencies at large magnetic fields.

The deviation of g_{2-} from its weak coupling value is an indication of the important role of ^3He quasiparticle and

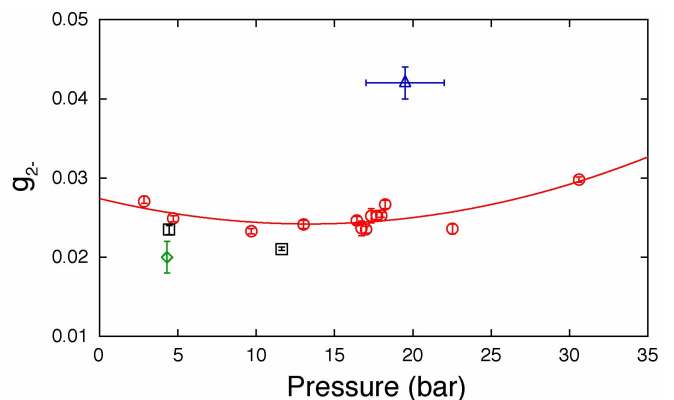


FIG. 4: (color online). The Landé g -factor, g_{2-} , as a function of pressure at $T = 0$. The red circles are from Faraday rotation measurements as a function of temperature, extrapolated to zero temperature. The black squares are measurements performed via pressure sweeps at our lowest temperatures. The blue triangle is from Movshovich *et al.* [16] and the green diamond is from Lee *et al.* [6]. The curve is given by $g_{2-} = 0.0274 - 4.8 \times 10^{-4} P + 1.8 \times 10^{-5} P^2$.

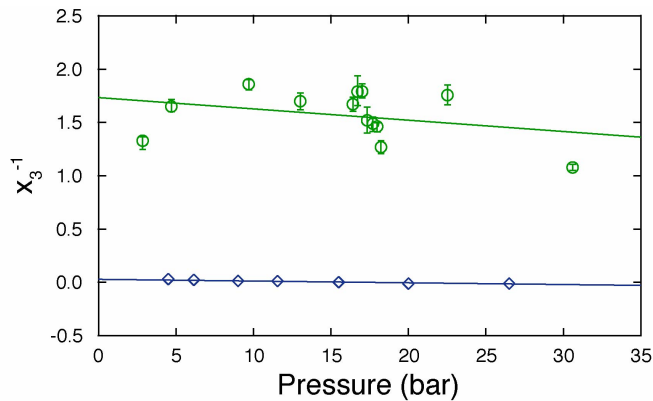


FIG. 5: (color online). The green circles are the f -wave interaction strength x_3^{-1} as function of pressure obtained from measurements of the ISQ-mode g -factor and frequency measurements and the blue diamonds are from ISQ-mode frequency measurements alone [7]. The solid lines are guides to the eye. The significant difference between these two data sets is likely associated with strong coupling effects on the ISQ-mode frequencies, discussed in the text.

pairing interactions. According to the theory of Sauls and Serene [8] the two relevant parameters are the Landau parameter F_2^s , and the strength of f -wave pairing interactions, $x_3^{-1} = 1/(v_1^{-1} - v_3^{-1})$. Here v_1 and v_3 are the pairing potentials due to p -wave and f -wave interactions respectively. The theory allows calculation of x_3^{-1} from g_{2-} and the zero-field ISQ-mode frequencies, with F_2^s and the energy gap as inputs. We use values for F_2^s , based primarily on measurements of the difference between zero- and first-sound velocities in the normal fluid, and Δ^+ as tabulated in Ref. [9]. The theoretical expression for g_{2-} is complex and is not reproduced here. The green circles in Fig. 5 show the result of this calculation, with all predicted dependences on these parameters including the explicit dependences of Λ_{2-} and Λ_0 on F_2^s .

We find that x_3^{-1} is positive, which means that f -wave interactions are repulsive, with little pressure dependence. These values are in disagreement with our results from analysis of the ISQ-mode frequencies [7], interpreted within the framework of Ref. [17], shown as blue diamonds in Fig. 5. We believe that the discrepancy between these two calculations of x_3^{-1} likely originates in non-trivial strong coupling corrections to the ISQ-mode frequencies. For example, at 5 bar our measurements reveal that Fermi liquid and f -wave corrections to the mode frequencies are $\lesssim 0.9\%$, whereas strong coupling corrections to Δ are 2.5%. This situation persists at all pressures, suggesting that calculations of the mode frequencies beyond the weak-coupling-plus model [13] are required. On the other hand the g -factor is more strongly modified by interaction effects as compared with the mode-frequency and so x_3^{-1} derived from the g -factor should be more robust. Variation of the absolute temperature scale by 1 % and F_2^s by 0.5 have negligible effect on the calculation of the g -factor and change x_3^{-1} within the scatter of the data.

One of the predictions of Sauls and Serene [17] is that for some combination of either negative values of x_3^{-1} or a negative higher order Landau interaction term, F_4^s , there is a new order parameter collective mode close to the gap edge that corresponds to total angular momentum $J = 4$. Longitudinal sound attenuation measurements [18] near $\omega = 2\Delta$ were initially interpreted in this way although this was later revised as providing evidence for a $J = 1$ collective mode. Acoustic Fourier transform spectroscopy [19] indicated an unexplained additional contribution to attenuation near the gap and an explanation in terms of the $J = 4$ mode was also considered. It should be possible to use high resolution acoustic cavity methods, as in the present work, to look for these modes although our determination of the repulsive interaction in the f -wave channel is not encouraging.

In summary, we have investigated the magneto-acoustic Faraday effect in superfluid ^3He using high resolution transverse sound techniques. Our spectroscopic data for the ISQ-mode frequency and its g -factor are the most complete characterization of an order parameter collective mode in superfluid ^3He . We find from our results, combined with the theory, that f -wave pairing interactions are repulsive. But strong-coupling corrections to the ISQ-mode frequencies may be required to understand the full effect of f -wave interactions on the collective modes.

We acknowledge support from the National Science Foundation, DMR-0703656 and thank J.A. Sauls, T.M. Lippman, W.J. Gannon, and B. Reddy for useful discussions and Y. Lee and G. Gervais for early contributions.

-
- [1] C. Kittel, Phys. Rev. **110**, 836 (1958).
 - [2] H. Matthews and R.C. LeCraw, Phys. Rev. Lett. **8**, 397 (1962).
 - [3] M. Boiteux *et al.*, Phys. Rev. B **4**, 3077 (1971).
 - [4] D. Dominguez, *et al.*, Phys. Rev. Lett. **74**, 2579 (1995).
 - [5] G.F. Moores and J.A. Sauls, J. Low Temp. Phys. **91**, 13 (1993).
 - [6] Y. Lee *et al.*, Nature **400**, 431 (1999).
 - [7] J.P. Davis, *et al.*, Phys. Rev. Lett. **97**, 115301 (2006).
 - [8] J.A. Sauls and J.W. Serene, Phys. Rev. Lett. **49**, 1183 (1982).
 - [9] W.P. Halperin and E. Varoquaux, in *Helium Three*, ed. by W.P. Halperin and L.P. Pitaevskii (Elsevier, Amsterdam 1990).
 - [10] J.A. Sauls, cond-mat/9910260.
 - [11] P.J. Hamot, H.H. Hensley, and W.P. Halperin, J. Low Temp. Phys. **77**, 429 (1989).
 - [12] J.P. Davis *et al.*, to be published.
 - [13] D. Rainer and J.W. Serene, Phys. Rev. B **13**, 4745 (1976).
 - [14] D.S. Greywall, Phys. Rev. B **33**, 7520 (1986).
 - [15] N. Schopohl and L. Tewordt, J. Low Temp. Phys. **45**, 67 (1981).
 - [16] R. Movshovich, E. Varoquaux, N. Kim, and D.M. Lee, Phys. Rev. Lett. **61**, 1732 (1988).
 - [17] J.A. Sauls and J.W. Serene, Phys. Rev. B **23**, 4798 (1981).
 - [18] R.H. Ling, J. Saunders, and E.R. Dobbs, Phys. Rev. Lett. **59**, 461 (1987).
 - [19] N. Masuhara, B. C. Watson, and M.W. Meisel, Phys. Rev. Lett. **85**, 2537 (2000).